BASIC SCIENCE

Nanomedicine: Nanotechnology, Biology, and Medicine
14 (2018) 1137–1148

nanomedicine
Nanotechnology, Biology, and Medicine

Original Article

nanomedjournal.com

Enhancing glioblastoma treatment using cisplatin-gold-nanoparticle conjugates and targeted delivery with magnetic resonance-guided focused ultrasound

Daniel Coluccia, MD[a,1], Carlyn A. Figueiredo, MSc[a,b,1], Megan YiJun Wu, MSc[a], Alexandra N. Riemenschneider, BSc[a], Roberto Diaz, MD, PhD[a], Amanda Luck, BSc[a], Christian Smith, PhD[a], Sunit Das, MD, PhD[a,b], Cameron Ackerley, PhD[b], Meaghan O'Reilly, PhD[c], Kullervo Hynynen, PhD[c], James T. Rutka, MD, PhD, FRCSC[a,b,*]

[a]*Division of Neurosurgery, the Arthur and Sonia Labatt Brain Tumor Research Centre*
[b]*Division of Laboratory Medicine and Pathobiology, the Hospital For Sick Children*
[c]*Sunnybrook Health Sciences Centre Research Institute, the University of Toronto*

Received 6 August 2017; accepted 29 January 2018

Abstract

Glioblastoma (GBM) is the most common and aggressive primary brain tumor resulting in high rates of morbidity and mortality. A strategy to increase the efficacy of available drugs and enhance the delivery of chemotherapeutics through the blood brain barrier (BBB) is desperately needed. We investigated the potential of Cisplatin conjugated gold nanoparticle (GNP-UP-Cis) in combination with MR-guided Focused Ultrasound (MRgFUS) to intensify GBM treatment. Viability assays demonstrated that GNP-UP-Cis greatly inhibits the growth of GBM cells compared to free cisplatin and shows marked synergy with radiation therapy. Additionally, increased DNA damage through γH2AX phosphorylation was observed in GNP-UP-Cis treated cells, along with enhanced platinum concentrations. *In vivo*, GNP-UP-Cis greatly reduced the growth of GBM tumors and MRgFUS led to increased BBB permeability and GNP-drug delivery in brain tissue.

Our studies suggest that GNP-Cis conjugates and MRgFUS can be used to focally enhance the delivery of targeted chemotherapeutics to brain tumors.

Key words: Glioblastoma; Gold nanoparticles; Target delivery; Focused ultrasound

Glioblastoma (GBM) is the most common and aggressive primary brain tumor.[1] Even following maximum resection, radiation therapy (RT) and chemotherapy, the median survival is only 15 months.[2] Within the capillary bed of the brain parenchyma, the movement of ions, molecules and cells is highly regulated via the BBB, posing a major obstacle for obtaining effective drug concentrations within the tumor.[3,4] Hence, adequate penetration of therapeutic agents is only achievable at higher systemic doses, carrying potentially intolerable side effects and limiting the usefulness of most well-established cancer drugs.[3] Direct deposition of BCNU-wafers in the tumor resection cavity might improve local tumor control without inherent systemic toxicity; however repeated application and long term disease control are limited.[5] Temozolomide (TMZ) is the only orally administered chemotherapeutic agent which has convincingly proven to prolong

The authors declare no conflict of interest.

Funding: This work was supported by grants from the Canadian Institutes of Health Research (CIHR) MOP 74610 and 377975, b.r.a.i.n.child, Meagan's Walk Foundation, the Laurie Berman Fund for Brain Tumor Research, and the Wiley Family Fund.

*Corresponding author at: Division of Neurosurgery, Suite 1503, The Hospital for Sick Children, 555 University Avenue, Toronto, Ontario, Canada M5G 1X8.
E-mail address: james.rutka@sickkids.ca (J.T. Rutka).

[1] These authors contributed equally to this study.

https://doi.org/10.1016/j.nano.2018.01.021
1549-9634/

survival of GBM patients, but only by about 2 months.[2] Cisplatin (Cis) is one of the most commonly used and effective anti-cancer drugs with well-described cytotoxic effects, and is a known radio-sensitizer.[6,7,8] However, high doses of Cis are often needed to penetrate the BBB, which often involve intolerable systemic adverse effects.[7] Additionally, about 90%-95% of Cis becomes irreversibly bound to plasma proteins, leaving only 5%-10% of the drug fraction free to exert anti-tumor effects.[9,10]

One strategy to alter drug effects is to use gold nanoparticles (GNPs) as carriers and modifiers, offering the potential for targeted and increased delivery without redesigning a drug's molecular structure.[11] GNPs have gained increasing interest as modifiers of conventional drugs, in addition to their role as radiosensitizers.[12] Moreover, they are already being used in FDA approved clinical trials.[13,14] GNPs can reliably be produced at different sizes and shapes. Their highly tunable surfaces allow various coatings to increase biocompatibility and facilitate functionalization for diagnostic and therapeutic purposes.[11]

GNPs have repeatedly been shown to enter tumor cells and markedly accumulate in cancer tissue.[15,16] However, the infiltrative zone of brain tumors, as the most common site of tumor recurrence, demonstrates an intact BBB and prohibits significant GNP transfer.[17] We have previously demonstrated that by using focused ultrasound (FUS), functionalized GNPs can traverse the cerebral capillaries into the normal brain parenchyma.[18,19] In this study, we evaluated the use of GNP-bound Cis as a possible strategy to increase drug efficacy and growth inhibition in experimental GBM. To treat the infiltrative tumor zone, we further assessed the usefulness of targeted non-invasive Magnetic Resonance-guided Focused Ultrasound (MRgFUS) to transiently disrupt the otherwise intact BBB and increase the GNP-drug delivery.

Methods

GBM cell lines

All cells were cultured at 37°C and 5% CO_2. Human GBM cell lines (U87, U251, T98G, U138) were grown in Dulbecco's Modified Eagle Media (DMEM) + 10% Fetal Bovine Serum (FBS) (Wisent Inc.).

Gold nanoparticles

Size-certified 7 nm spherical gold nanoparticles (GNPs) coated with polyacrylic acid (PAA) were purchased from Nanopartz ™ (Loveland, CO). Four different GNP compounds were applied: Non-functionalized GNPs (D11-10-NC-Bulk), GNPs functionalized with Cis (GNP-Cis) (DRE11-10-CIS-50), GNPs functionalized with a cell uptake peptide (GNP-UP) (PKKKRKV, SV40 antigene, nuclear localization signal, DRE11-10-CU-50),[22,23] and GNPs with uptake peptide (UP) conjugated with Cis (GNP-UP-Cis) (DRE11-10-CIS-CU-50). A covalently bonded porous polymer was used as the backbone for loading the cisplatin through ionic adsorption. This provided an optimized loading efficiency in a polymer that only adds 1-2 nm in diameter. In the constructs that include the cell uptake peptide, a mixed monolayer was used on the nanoparticles. Here the cisplatin was loaded using the scheme above, whereas the cell uptake peptide was covalently bound through a proprietary 8 carbon thiol based backbone. The colloidal gold solution was delivered at a pH of 7.0 containing an average of 1.70 E+15 nps/ml (Molarity 2.71 μM). Functionalized GNPs carried an estimated 375 cisplatin molecules and/or 350 uptake polypeptides per nanoparticle. TEM images were provided by Nanopartz™ to verify that nanoparticles were not aggregated (Figure S1, *D*). Zeta potential at pH 7 ranged from −35 mV (non-functionalized) to + 15mV (GNP-UP-Cis). (Figure S1 and S2).

Cell viability assays

Alamar blue cell viability assay (Invitrogen) was used to assess drug toxicity to GBM cells. Cells were plated into 96-well dishes at a density of 2000 cells/well, using 6 wells as replicates for each condition for statistical analysis. Drug was incubated for 1 to 6 days. For radiation treatment, cells were incubated for 24 h with drug/GNP and exposed to 6 Gy. Viability was assessed 1 day after radiation treatment.

Assessment of cell uptake of Cis

0.1×10^6 cells/well of U251 and U87 cells were exposed to a low dose, non-toxic concentration of 0.33 μM cisplatin for 2 h, 4 h, and 12 h (n = 3 wells for each condition). Cells were detached and pelleted into a 1.5 ml Eppendorf tube. The cell pellet was dissolved in aqua regia (3:1 HCL/HNO3) in borosilicate glass tubes. After dilution in milliQ water the platinum content was analyzed by inductively coupled mass spectroscopy (ICP-MS, PerkinElmer NexION 300/350i).

Confocal microscopy

Cells were exposed to saline, Cis, GNP-UP, or GNP-UP-Cis for 48 h, fixed with 4% PFA and permeabilized with 0.5% Triton X-100. 5% BSA block was applied for 1 h at 37 °C. Incubation with the primary antibody (γH2AX 1:1000 Millipore) was performed overnight at 4 °C and secondary antibody (Alexa-488, 1:500 Abcam) for 1 h at room temperature. Actin was stained with Phalloidin-594 (ThermoFisher Scientific) and nucleus with DAPI (Vectashield Mounting Medium). Cellular localization of GNP was imaged using silver enhancement staining (Cytodiagnostics). Images were captured using Zeiss LSM700 and quantified with ImageJ software. The area ratio γH2Ax/DAPI was calculated using Volocity 6.3 software, analyzing at least 60 cells per condition at 20× magnification.

Transmission electron microscopy (TEM)

5×10^6 U251 cells were seeded in 10 cm^2 dishes and incubated with GNP-UP-Cis (ratio of 4×10^6 nanoparticles: 1 cell) overnight. Dissociated cells were fixed in 250 μL of 2% glutaraldehyde in 0.1 M sodium cacodylate buffer pH 7.3 for 1 h at room temperature. Samples were post-fixed in 1% osmium tetroxide in buffer, dehydrated in a graded ethanol series followed by propylene oxide, and embedded in Quetol-Spurr resin. Sections 100 nm thick were cut on an RMC MT6000 ultramicrotome, stained with uranyl acetate and lead citrate and viewed in an FEI Tecnai 20 electron microscope (Hillsboro, OR).

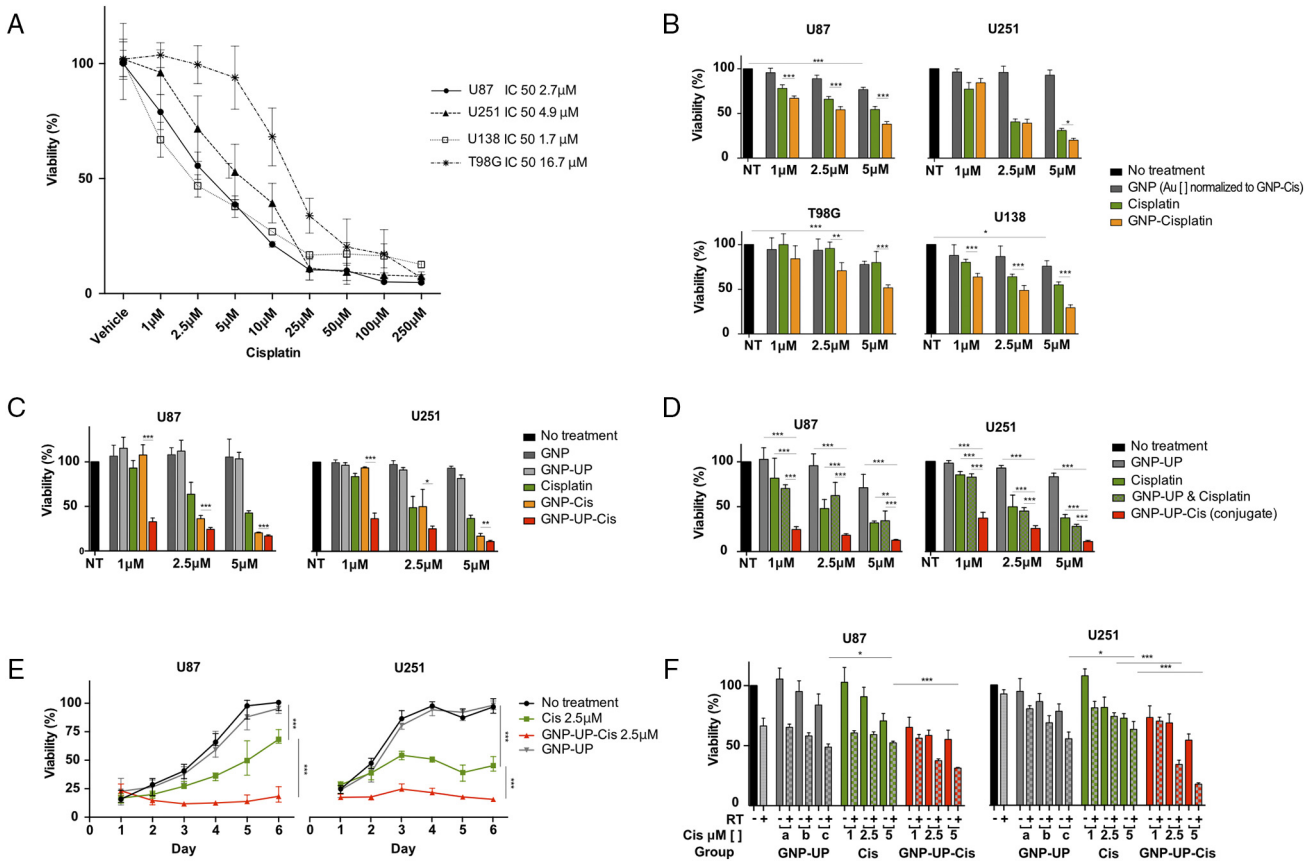

Figure 1. *In vitro* results of GNP testing on different GBM cell lines. (A) Growth inhibition observed in all cell lines. IC50 ranging between 1.7 and 16.7 μM.(B) GNP-Cis shows an increased growth inhibition when compared to Cis alone at all tested concentrations in slow-duplicating GBM cell lines (U87, U138), and at higher concentrations for fast-duplicating cell lines (U251, T98G). (C) Functionalization with uptake peptide (GNP-UP-Cis) further increased dose-dependent growth inhibition when compared to GNP-Cis and Cis alone. (D) GNP-UP-Cis exhibited a significantly stronger cell inhibitory effect compared to an equivalent mixture of unconjugated GNP-UP and Cis. (E) Enhanced inhibition of cell proliferation by GNP-UP-Cis was sustained over several days when compared to Cis alone. (F) Effect of RT and GNP-UP-Cis on two cell lines (A) U87 and (B) U251. The synergistic cytotoxic effect of RT and non-functionalized GNPs exceeded the response found with RT and Cis when administered by themselves. Growth inhibition was further amplified when GNP-UP-Cis was used. Equivalent concentrations of GNPs were used as that found in 1 μM (a), 2.5 μM (b) and GNP-UP-Cis (c). One-way ANOVA with Tukey post-hoc analysis, $P<0.05$*, $P<0.01$**, $P<0.001$***.

Orthotopic xenotransplantation of GBM

All animal procedures were approved by the Animal Care Committee at Sick Kids Hospital Research Institute, Toronto Centre for Phenogenomics (TCP) and Sunnybrook Health Sciences Centre. Animal-use-protocols are in accordance with the guidelines established by the Canadian Council on Animal Care and the Animals for Research Act of Ontario, Canada.

NOD SCID Gamma (NSG) female mice were injected with 0.5×10^6 U251-Luc cells (see Supplementary Methods for characteristics of U251-Luc) into the right frontal lobe. Mice were randomized to one of four treatment arms: Saline (n=4), GNP-UP (n=4), Cis (n=5), GNP-UP-Cis (n=6). Bioluminescence (Perkin Elmer, IVIS Spectrum Optical In-vivo Imaging System) images were taken at day 9 after cell implantation and treatments were initiated on day 10. A total of 5 intravenous injections were given every other day: GNP-UP (2.46 μM Au), Cis (1.5 mg/kg) and GNP-UP-Cis (1.5 mg/kg cisplatin; 2.46 μM Au). Mice were sacrificed when 15% of body weight was lost or when neurological or behavioral impairment was observed. Images were analyzed using the software Living Image 4.5 (PerkinElmer).

Histological and immunohistochemistry (IHC)

Hematoxylin and Eosin (H&E) staining was used to determine the histopathological features. Ki67 (Abcam 1:1500) and Caspase 3 (Cell signaling 1:1000) were used to evaluate tumor cell proliferation and apoptosis respectively. A silver enhancement kit (Ted Pella) was used to visualize distribution of GNPs in tissues. Sections were imaged using a 3D Histech Pannoramic 250 slide scanner. Ki67 and Caspase 3 was quantified with 3D Histech Pannoramic Image Analysis Software, using a colorimetric algorithm to calculate the percentage of positive pixels over a designated tissue area, defined as relative mask area (rMA).

Tumor targeting with MRgFUS

NSG mice were anesthetized with isofluorane and placed supine in a mount for transcranial sonication and MR imaging (Figure S4). The exposed scalp was positioned on a gel pad overlying a well, filled with degassed water allowing coupling of acoustic waves (See Supplementary Methods). Prior to sonication, animals were injected with 0.02 ml/kg of lipid-coated

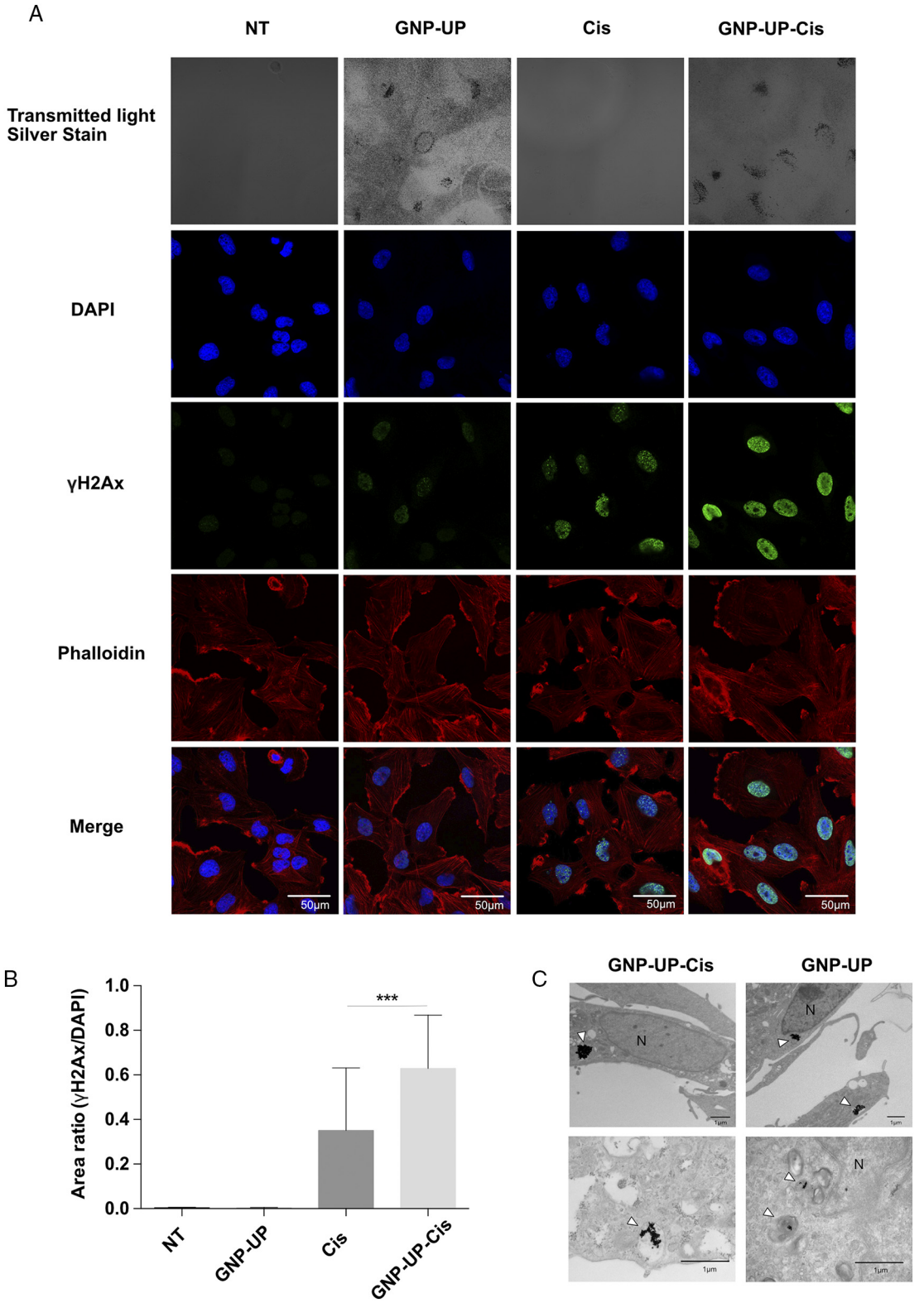

Figure 2. Assessment of efficacy of GNP-UP-Cis through immunofluorescence and electron microscopy in U251 GBM cells. (A) Confocal IF microscopy showing GNP internalization via silver stain (transmitted light), along with staining for DAPI to show nuclei (blue), γH2AX for DNA damage (green) and phalloidin for actin filaments (red). An increase in the phosphorylation of γH2AX in cells treated with GNP-UP-Cis was observed, compared to Cis alone. No change in cell morphology and only minor γH2AX foci could be detected in cells exposed to drug-free GNP-UP. (B) Quantification of positive γH2AX cells showed an increase in the relative DNA damage of cells treated with GNP-UP-Cis compared to drug alone (one way ANOVA with Tukey post hoc analysis, $P<0.001$***). (C) TEM of U251 cells showed that both GNP-UP-Cis and GNP-UP were located in perinuclear vesicular organelles (arrow head) without any apparent GNPs in the nucleus (N).

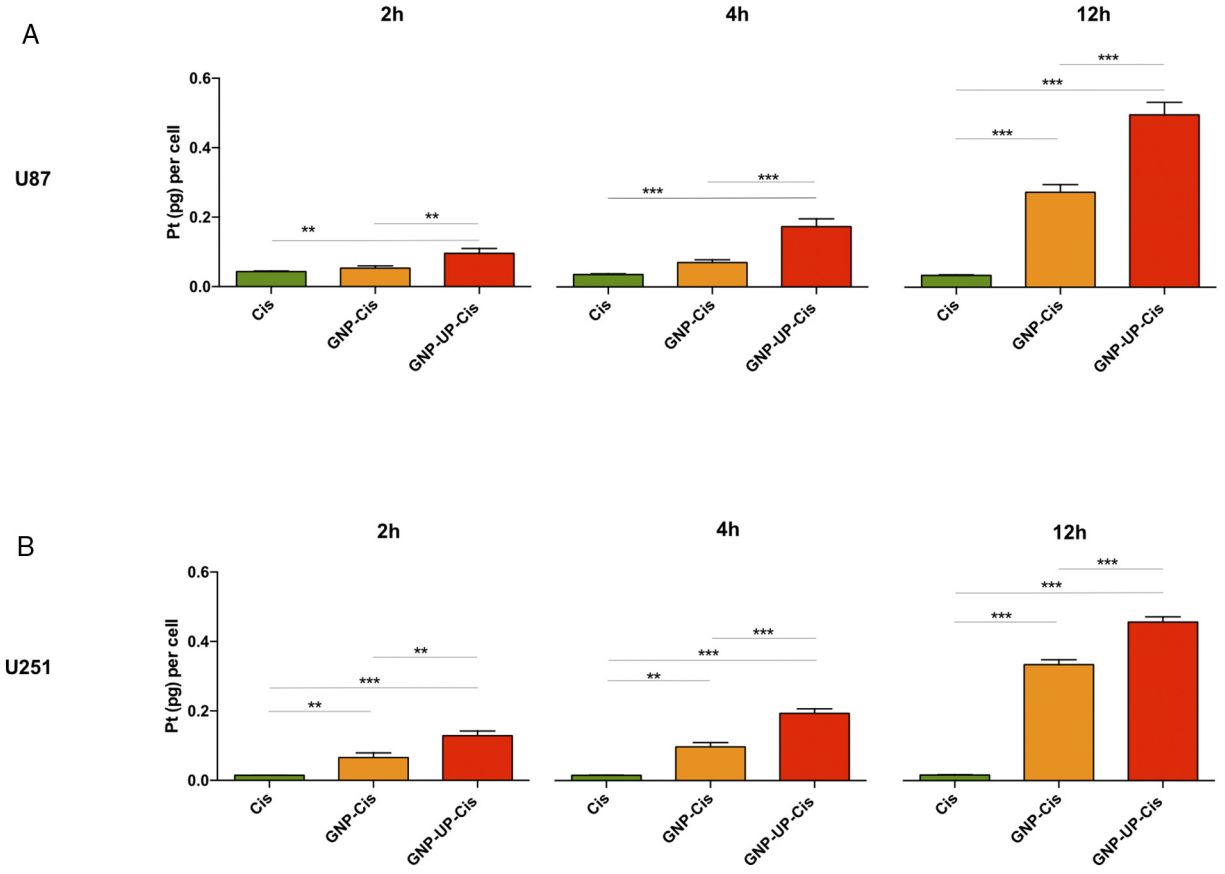

Figure 3. Concentration of internalized Cis quantified by ICP-mass spectrometry in (A) U87 and (B) U251. GBM cells were exposed to cisplatin, GNP-Cis or GNP-UP-Cis for 2 h, 4 h and 12 h. Both GNP-Cis conjugates showed an increasing drug (Pt) uptake over time when compared to Cis alone, while adding the uptake peptide resulted in enhanced uptake for GNP-UP-Cis (one-way ANOVA with Tukey post hoc analysis, $P<0.01$**, $P<0.001$***).

echogenic microbubbles (Definity, Lantheus Medical Imaging, Saint-Laurent, Québec) via tail vein followed by either Cis (0.5mg/kg) or GNP-UP-Cisplatin (0.5 mg/kg). Subsequently, gadolinium 0.1 ml/kg (Gadovist) was injected followed by 0.2 ml saline flush. For localized BBB-disruption, a spherically focused transducer (1.68 MHz, 75 mm aperture, focal-number = 0.8) was used with standard BBB opening parameters (10-ms bursts, 1-Hz burst repetition frequency, 120 s duration).[20] The acoustic pressure was modulated burst to burst during the 120 s sonication based on the detection of sub and ultraharmonic microbubble emissions, as previously described.[18] Contrast-enhanced T1-weighted images (500/10) were used to confirm BBB opening. 24 h after injection/sonication, the animals were deeply anesthetized with ketamine/xylazine and blood samples were collected via cardiac puncture. All animals were perfused with 0.9% saline prior to the harvesting of organs (brain, liver, kidney, and spleen). The platinum (for cisplatin) and gold content was analyzed by inductively coupled mass spectroscopy (ICP-MS, PerkinElmer NexION 300/350i).

Results

Characterization of GBM cell line sensitivity to Cis and GNP-Cis

The sensitivity of GBM cells to Cis was assessed in 4 different human GBM lines: U251, T98G, U87, and U138. All cell lines showed a dose dependent inhibition of growth with the IC50 ranging from 1.7 to 16.7 μM Cis (Figure 1, *A*). Cells were then exposed to Cis, GNP, or GNP-Cis, at equivalent doses of Cis and GNP respectively. The GNP-Cis compound revealed significantly higher dose-dependent growth inhibition when compared to Cis alone (Figure 1, *B*). At higher concentrations, non-functionalized GNPs also showed slight growth inhibition, consistent with previous studies showing that unmodified GNPs can inhibit proliferation of cancer cells. [15,21] Aiming to further enhance the efficacy of the GNP drug compounds, we functionalized the nanoparticles with an uptake peptide (GNP-UP-Cis). GNP-UP-Cis showed a distinctively increased, dose-dependent growth inhibition compared to GNP-Cis and Cis alone (Figure 1, *C*). The IC50 of GNP-UP-Cis of U87 and U251 was markedly below 1 μM and showed higher levels of toxicity when compared to GNP. We repeated the same experiment with a mixture of GNP-UP and Cis at an equivalent concentration to GNP-UP-Cis to assess whether the observed cell response to GNP-UP-Cis was a result of separate effects of functionalized GNP and Cis. The results show that the increased effect of GNP-UP-Cis cannot solely be explained by separate actions of GNP-UP and Cis and that GNP-UP-Cis acted as a distinct entity (Figure 1, *D*). Furthermore, enhanced inhibition of cell proliferation by GNP-UP-Cis was sustained over several days at a greater degree than Cis alone (Figure 1, *E*).

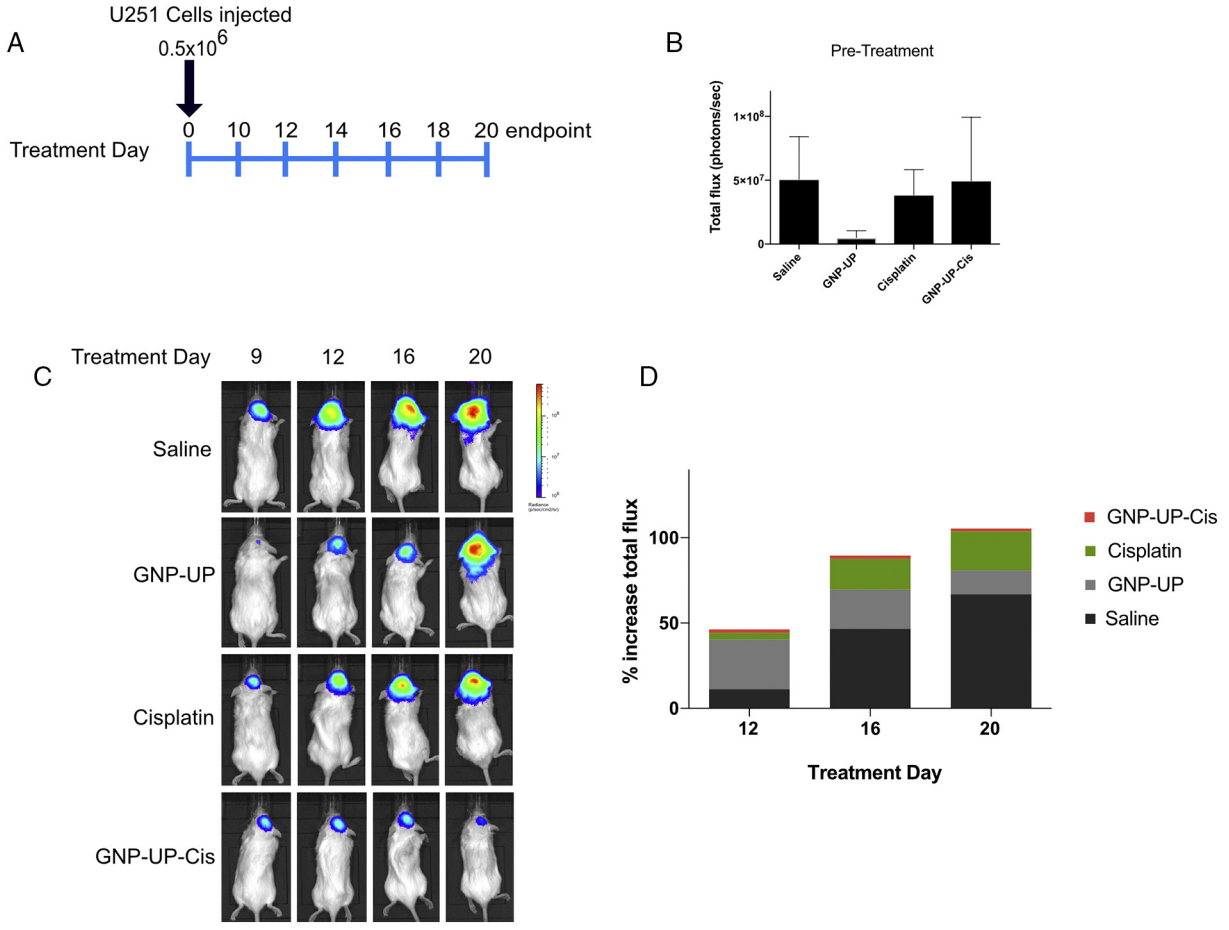

Figure 4. Orthotopic GBM brain tumor mouse model to assess therapeutic properties of GNP-UP-Cis in *vivo*. Stereotactic implantation of luciferase transfected U251 cells in the right frontal lobe. (A) Timeline demonstrating the intracranial injection of U251-Luc cells followed by the treatments. (B) Total flux measured before treatment. (C) Bioluminescence imaging of tumors at Day 9 pre-treatment and on treatment days 12, 16 and 20. (D) Percent increase of total flux measured of tumors on treatment days 12, 16 and 20, relative to Day 9 pre-treatment measurement showing markedly higher flux increase for saline vs. GNP-UP-Cis, most notably on treatment day 20 (one-way ANOVA with Tukey post hoc analysis, $P<0.05$*).

Effects of RT on GBM cell lines

As both Cis and GNPs are recognized as radiosensitizing agents,[7,12] we examined whether the superior cell inhibition of GNP-UP-Cis was retained when cells were exposed to ionizing radiation. The synergistic effect of radiotherapy and Cis-free GNPs exceeds the response found with Cis alone (Figure 1, *F*). Growth inhibition was further amplified when GNP-UP-Cis was used.

GNP-UP-Cis versus Cis in inducing DNA damage

Western blot analysis confirmed the expression of γH2AX in GBM cells exposed to higher doses of Cis (Figure S5, *A*). In comparison, GNP-UP-Cis was more effective in inducing DNA damage and cell apoptosis than Cis and GNP-Cis (Figure S5, *B*). Drug free GNP and GNP-UP did not affect cellular DNA during the time of exposure, as inferred by the absent upregulation of p53. Confocal IF microscopy confirmed the increased phosphorylation of γH2AX in cells treated with GNP-UP-Cis (Figure 2, *A* and *B*). No change in cell morphology and no increased γH2AX foci were apparent when non-functionalized GNPs were used. We conclude that GNPs themselves did not significantly alter cell homeostasis during the time of exposure.

Intracellular GNP localization

As indicated by silver staining (Figure 2, *A*), GNP-UP-Cis particles accumulated around the nucleus and were undetected within the nucleus itself. This was confirmed by TEM, which showed that both GNP-Cis and GNP-UP-Cis were located in perinuclear vesicular organelles (Figure 2, *C*). Therefore, the observed superior efficacy of GNP-UP-Cis over GNP-Cis cannot be explained by a more direct drug deposition into the nucleus. DNA damage was only appreciated when cells were exposed to GNP-UP-Cis and not to GNP-UP (Figure 2, *A*), and GNP-UP-Cis has been shown to be more efficacious than a mixture GNP-UP + Cis (Figure 1, *D*).

Cellular internalization of Cis

To determine the time-dependent cell uptake of Cis for GNP-Cis, GNP-UP-Cis and Cis alone, platinum (Pt) content

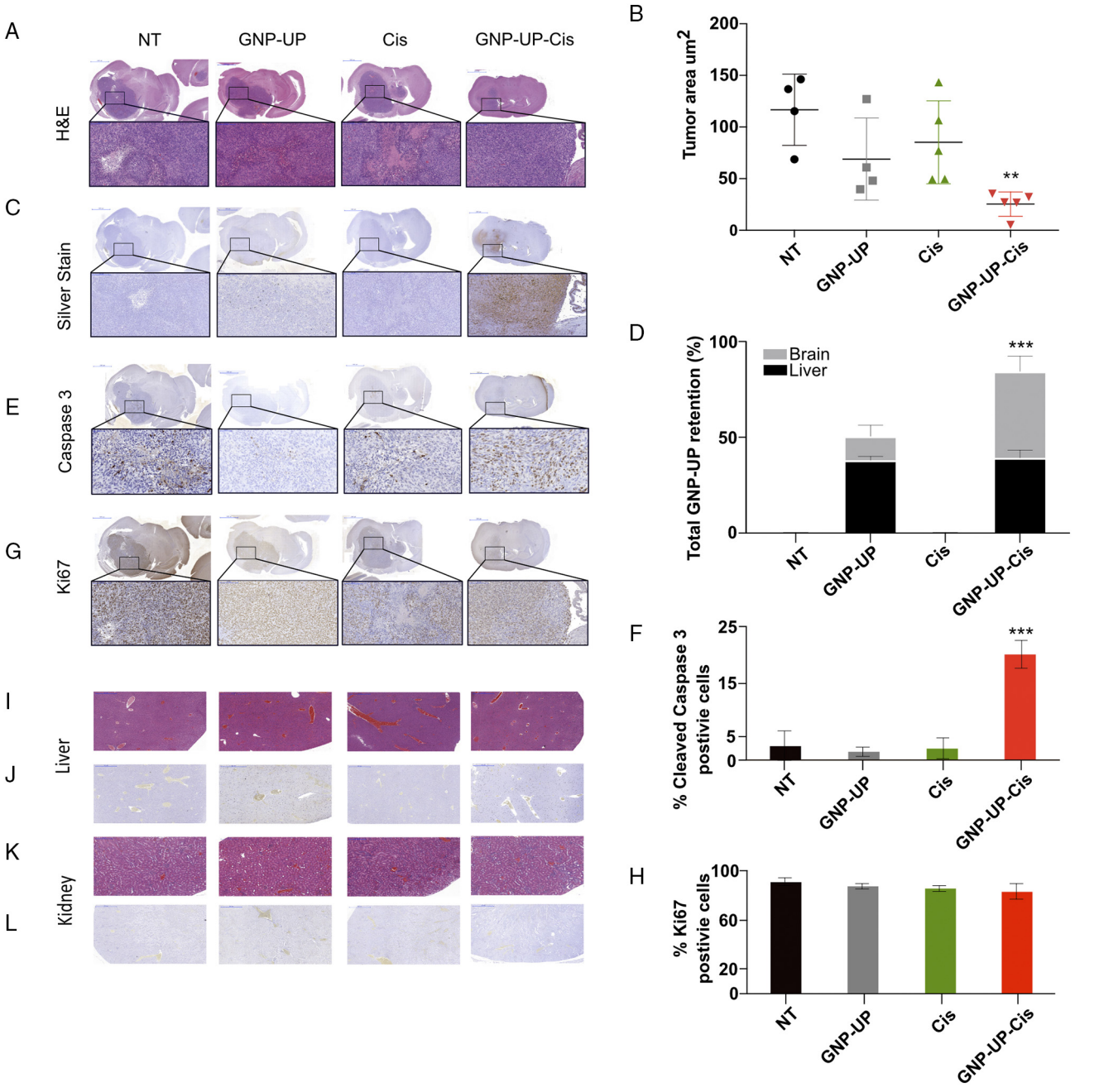

Figure 5. Histological effects of drug treatments on GBM xenografts: (A) Representative H&E images of brains after 5 treatments showing the histological features of U251 GBM xenograft. (B) Quantification of tumor size as from coronal H&E sections. Statistical analysis via two-tailed t test, GNP-UP-Cis vs other groups. (C) Light microscopic images of silver-enhanced stained sections showing the distribution of GNPs in brain tumors. (D) Quantification of positive area of silver staining in the brain relative to the entire tumor area. Measurements are also reported for the liver relative to entire liver section. Mean ± S.D., two-tailed t test, brain GNP-UP-Cis vs GNP-UP. (E) IHC staining shows significant increase in the number of apoptotic Cleaved Caspase 3 positive cells in the tumor region. (F) Graph shows quantification of immuno-positive cells for cleaved Caspase 3 relative to cell number in entire tumor region. Mean ± S.D., two-tailed t test, GNP-UP-Cis vs the rest of groups. (G) IHC staining shows high expression of Ki67 in tumors. (H) Quantification of Ki67 positive cells relative to entire tumor region. Mean±S.D., two-tailed t test, GNP-UP-Cis vs the rest of groups, $P>0.1$ NS. (I) Representative H&E images of liver after treatments. (J) Silver-enhanced stained liver sections showing nanoparticle distribution. (K) Representative H&E images of kidneys after treatments. (L) Silver-enhanced stained kidney sections showing no apparent intraparenchymal nanoparticle distribution.$P<0.01$**, $P<0.005$***.

within the cells was assessed by ICP-MS. As shown in Figure 3, no increase of Pt internalization of cells exposed to Cis could be detected after 2 h, indicating a steady state between the medium and the intracellular compartment. Both GNP-Cis conjugates showed a higher drug uptake when compared to Cis alone. Interestingly, GNP-UP-Cis shows the highest uptake, reflecting the higher cell toxicity as previously shown (Figure 1).

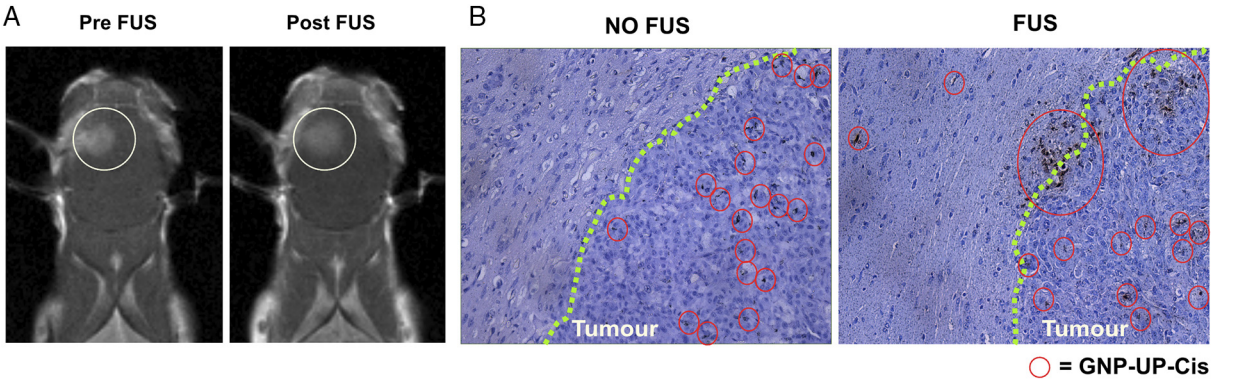
A
Pre FUS
Post FUS
B
NO FUS
FUS
Tumour
Tumour
= GNP-UP-Cis

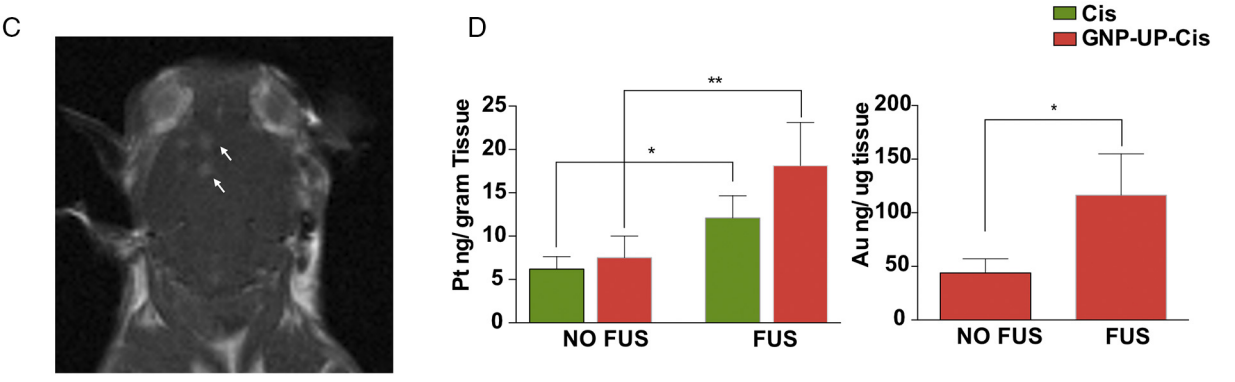
C
D
Cis
GNP-UP-Cis
Pt ng/ gram Tissue
25
20
15
10
5
0
**
*
NO FUS
FUS
Au ng/ ug tissue
200
150
100
50
0
*
NO FUS
FUS

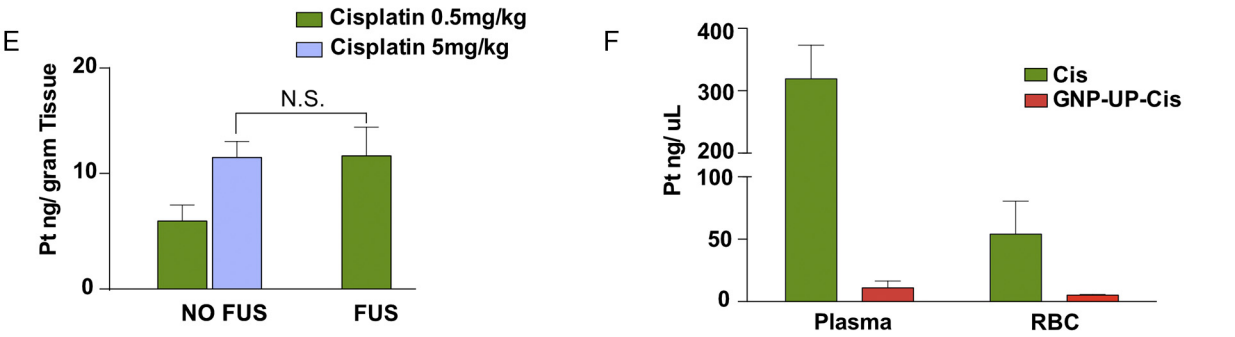
E
Cisplatin 0.5mg/kg
Cisplatin 5mg/kg
Pt ng/ gram Tissue
20
10
0
N.S.
NO FUS
FUS
F
Pt ng/ uL
400
300
200
100
50
0
Cis
GNP-UP-Cis
Plasma
RBC

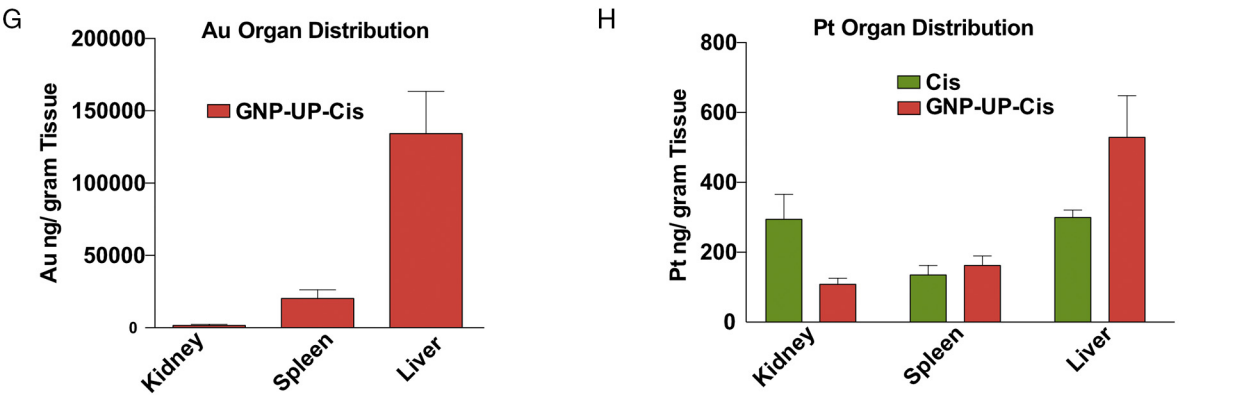
G
Au Organ Distribution
Au ng/ gram Tissue
200000
150000
100000
50000
0
GNP-UP-Cis
Kidney
Spleen
Liver
H
Pt Organ Distribution
Pt ng/ gram Tissue
800
600
400
200
0
Cis
GNP-UP-Cis
Kidney
Spleen
Liver

GNP-UP-Cis inhibits GBM growth in vivo

Ten days after tumor implantation, animals were treated with IV injection of therapeutic compounds. Animals were imaged between injections and sacrificed after 5 injections (Figure 4, *A*). Before treatment, GBM tumors did not significantly differ in size (Figure 4, *B*). Animals injected with saline showed the greatest tumor growth, followed by the GNP-UP and Cis group. Only tumors in animals treated with GNP-UP-Cis showed minimal to no tumor growth (Figure 4, *C* and *D*). H&E images revealed histological features of U251 GBM xenograft including necrosis, invasion and hypercellularity (Figure 5, *A* and *B*). Interestingly, GNP-UP-Cis treated mice demonstrated greater accumulation of GNPs within the tumor compared to GNP-UP treated animals (Figure 5, *C* and *D*), while both groups showed equivalent accumulation of GNPs in the liver (Figure 5, *D* and *J*). No GNPs were detectable in non-tumor brain tissue or in kidneys (Figure 5, *C* and *L*). Furthermore, GNP-UP-Cis treatment resulted in significant increase of activated Caspase 3 in the tumor tissue, in contrast to other treatment groups. Caspase 3 positive cells were diffusely distributed throughout the GNP-UP-Cis treated tumor, while in other treatment groups Caspase 3 positive cells were only found close to necrotic areas (Figure 5, *E* and *F*). There was however no significant difference in the expression level of mitotic activity across all treatment groups (Figure 5, *G* and *H*). No apparent morphological damage could be detected in the examined liver, kidney and spleen of animals treated with GNPs (Figure 5, *I* and *K*).

Increasing drug delivery with MRgFUS

MRgFUS induced increased Gd extravasation and thus increased BBB permeability at the tumor margin of sonicated mice (Figure 6, *A*). The animals did not show any neurological or behavioral sequelae from MRgFUS treatment. Histological samples revealed increased GNP deposition within the tumor and around the tumor margin with MRgFUS (Figure 6, *B*). In a second assessment, we sought to quantify the MRgFUS-induced increase of drug delivery compared to normal brain tissue with an intact BBB. MRgFUS requires increased volumes of fluid to be injected intravenously which includes microbubbles, drug, Gd, and flushes. As such, these may interfere with drug volumes in mouse models. Based on these limitations, we used a GNP-UP-Cis concentration of 0.5mg/kg and compared this with 0.5 mg/kg and 5 mg/kg Cis. We compared the Pt (drug) and Au (GNP) concentrations in the sonicated right frontal lobe versus the non-sonicated left frontal lobe (Figure 6, *C*). MRgFUS increased the Cis (Pt) and consequently the Au concentration in the brain 2-3.5-fold (Figure 6, *D*).

With MRgFUS, the tissue concentration achieved when using 0.5mg/kg Cis was comparable to the concentration achieved with 5 mg/kg cisplatin in the non-sonicated brain (Figure 6, *E*). The biodistribution of Cis was altered when bound on GNPs. ICP-MS analysis indicated that when conjugated to GNPs, there was no relevant binding of Pt to plasma proteins or red blood cells, as opposed to findings for free Cis injections (Figure 6, *F*). Given that protein-bound Cis is considered non-effective for tumor treatment, this finding may add to the explanation of higher tumor inhibition for the GNP bound Cis (Figures 4 and 5). GNP accumulation was highest in the liver and spleen (Figure 6, *G*), and therefore harbored the highest Pt load (Figure 6, *H*). Interestingly, using GNP-UP-Cis, the tissue concentration of Cis in the kidney was markedly lower when compared to injections with Cis alone (Figure 6, *H*). In our study, the histology of organs harvested after a total administration of 7.5mg/kg free and GNP-UP-Cis over 8 days showed no morphological alterations (data not shown).

Discussion

For most patients with GBM, current chemotherapies fail to substantially target the tumor and achieve long-term control. The development of new agents geared towards various molecular and genetic drivers is at an early stage with uncertain output.[37] Parallel efforts should be undertaken in optimizing the efficacy and delivery of well-established and successfully applied anticancer drugs.[31] We showed that Cis conjugated to GNPs offers a promising strategy to enhance tumor inhibition, while altering the systemic biodistribution of the drug and possibly improving biocompatibility. Increased inhibition of tumor growth by GNP-UP-Cis compared to Cis alone was confirmed *in vitro* and *in vivo*. In addition, MRgFUS successfully increased the drug delivery in the brain parenchyma with an intact BBB.

Previous studies have examined GNP-Cis, or related Pt-conjugates, in the treatment of other cancers. Kumar et al showed that a Pt-conjugated GNP had anti-cancer activity against prostate cancer cells *in vitro*, while Comenge et al studied the effect of Cis-conjugated GNPs in a mouse xenograft model of lung carcinoma.[32,38] Recently, Setua et al showed that a GNP-Cis conjugate could induce DNA damage and apoptosis in human GBM cells, and enhance radiotherapy-induced killing.[23] In Setua's study, the GNP-Cis conjugate synergized with radiotherapy more than control GNP particles. Thus, the combination of GNP-Cis with radiotherapy could prevent the emergence of radio-resistant clones.

Recently, Timbie et al[51] demonstrated that cisplatin-loaded nanoparticles up to 60 nm in diameter were capable of crossing the BBB using MRgFUS. Our work is in congruence with this study which demonstrates an enhanced delivery of cisplatin using nanoparticles and MRgFUS. However, to our knowledge, we present the first study using gold nanoparticles to

Figure 6. (A) Increased extravasation of Gd is observed post FUS (white circle) around tumor border. (B) Silver stained sections reveal increased GNP-UP-Cis (red circles) deposit within the tumor and around the tumor margin (green border) with FUS. (C) MRI imaging showing sonication in 4 spots in mouse right frontal lobe. Application of MRgFUS leads to Gd extravasation and thus BBB disruption (arrow). (D) Quantification of platinum (Pt) and gold (Au) amounts in brain tissue by ICP-MS following delivery of Cis (0.5 mg/kg) and GNP-UP-Cis (0.5 mg/kg) in the brain using MRgFUS. (E) Quantification of Pt showed an equal amount of cisplatin in brain tissue after 0.5 mg/kg of cisplatin and FUS, compared to 5 mg/kg of cisplatin. (F) A significantly reduced amount of cisplatin was measured to be bound to plasma and RBC with GNP-UP-Cis administration, as compared to Cis alone 24 h post treatment. (G) Au load was highest in the liver and spleen following GNP-UP-Cis administration. (H) Pt load corresponded to Au load following GNP-UP-Cis or Cis administration.

demonstrate efficacy of GNP-Cis conjugates in the treatment of GBM *in vitro* and *in vivo*. GNPs functionalized with Cis (GNP-Cis) showed superior inhibition of GBM cell growth *in vitro* compared to free Cis. By coupling GNPs to an uptake peptide and Cis (GNP-UP-Cis), we further increased the efficacy of GBM growth inhibition, DNA damage, and cell death. This enhanced efficacy appears to be due to the combined functional platform of the GNP-UP-Cis particle, and not the separate actions of GNP-UP and Cis.[33] Consistent with Setua's observations on radiotherapy, we confirmed the synergistic effect of GNP-UP-Cis with radiotherapy as an enhancement to inhibit growth of GBM cells.[24]

The uptake peptide (PKKKRKV) attached to GNP-UP-Cis is believed to increase nanoparticle internalization and to act as a nuclear localization signal (NLS).[22,23] Consistent with this, we found greater cell uptake of GNP-UP-Cis than either GNP-Cis or free cisplatin. However, we could not verify penetration of GNP-Cis or GNP-UP-Cis into the nucleus. In order to facilitate uptake into the nucleus, NLS has to bind to transport molecules such as importin, which enable entry through the nuclear pore complex.[39] To our knowledge, the potential for nuclear localization of PKKKRKV has not yet been assessed in GNPs conjugated with Cis. Therefore, it is possible that surface interactions between Cis and PKKKRKV might have impeded the binding of GNPs to transport molecules required for nucleus penetration. As demonstrated by our zeta-potential assessment (Figure S1), we hypothesize that the cationic surface charge on GNP-UP-Cis contributed to the increased cell internalization and that Cis is released from the GNP platform in the low pH environment of the late endosomes and/or lysosomes, and diffuses into the nucleus.[34]

In our *in vivo* models, GNP-UP-Cis showed minimal to no tumor growth, in striking contrast to treatment with saline, free Cis, and GNP-UP. Significant differences in uptake of the GNPs and distribution of apoptotic GBM cells within the tumor indicate that GNP-UP-Cis has a distinct functional activity when compared to GNP-UP or Cis. Notably, GNP-UP-Cis was well tolerated by mice as indicated by weight maintenance and intact behavior, and did not induce morphological alterations in any of the analyzed organs.

Given these promising results, future studies are needed to determine the long-term biocompatibility of such compounds, in terms of both altering the Cis load and accumulation of non-biodegradable Au in various organs. Ideally, GNPs should be designed to preferentially accumulate in tumor tissue while the excess is eliminated from the body. From various factors such as shape, coating and surface charge, GNP size is most crucial in determining renal clearance.[27,29,30] At a size less than 5-6 nm diameter, GNPs show efficient renal clearance, which prevents accumulation in the body and thus potential adverse long-term effects on healthy organs.[36] Then again, larger GNPs at sizes between 10 and 100 nm exhibit longer blood circulation time, which is favorable when aiming to increase the therapeutic efficacy of conjugated drugs.[40] Based on this observation, we chose smaller GNPs with an intermediate size of 7 nm in contrast to what has previously been published,[51] which offers some of the above-mentioned advantages regarding clearance and blood half time.[29]

As stated previously, the BBB presents a major obstacle to systemic drug delivery to the brain. Given that capillaries which arise from 'cancer induced neovascularization' show increased permeability, GNPs can penetrate and accumulate in most tumor tissue, including brain tumors.[15,16] However, in order to effectively treat brain tumors, the infiltrative zone, which is not amenable to surgical resection and where the highly selective BBB is more or less intact, has to be approached. We showed that MRgFUS could successfully permeabilize the BBB and increase delivery of both Cis and GNP-UP-Cis to normal brain tissue in the mouse. Future studies will evaluate the extent to which the FUS-induced boost of cisplatin and GNP-UP-Cis concentration translates into increased treatment effect on the tumor. However, our data are consistent with preclinical studies showing increased drug delivery with MRgFUS, and we hypothesize that increased drug delivery may lead to enhanced tumor control and prolonged survival in GBM models.[41–43] After FDA approval of ablative MRgFUS for procedures in patients with essential tremor and Parkinson disease[44] and following multiple animal studies attesting to the safety of repeated MRgFUS,[35,45] the first clinical trials on FUS-enabled drug delivery started in 2014.[46] High toxicity to GBM cells as noted in numerous *in vitro* studies together with Pt's demonstrably low BBB penetrance[25,26,47] makes well-known Pt-based agents ideal drugs to explore the usefulness of MRgFUS-induced drug delivery in brain tumors. In an ongoing phase I/IIa study on patients suffering from relapsing GBM, MRgFUS is being used to increase the delivery of carboplatin.[46] Preliminary results indicate that in patients with confirmed extended BBB opening, the region encompassed by the ultrasonic beam did not show tumor progression on follow-up MRIs at this early stage in the study.

Results from preclinical and clinical studies suggest that augmented drug delivery through MRgFUS offers great potential to enhance tumor growth inhibition and/or decrease adverse side effects, given that lower systemic dosage is needed to obtain equivalent concentration in the region of interest. In this regard, combining MRgFUS with drug carriers such as GNPs often exhibits an enhanced permeability and retention within the tumor along with longer circulation times compared to the free drugs.[28] This synergism allows the potential reduction in the frequency of drug administration. This is especially attractive when considering the marked radiosensitizing effect of GNPs, which is based on their strong absorption of ionizing radiation resulting in increased release of electrons and finally formation of reactive free radicals.[12,48]

Our results show the growth-inhibitory effects of Cis-conjugated GNPs in both *in vitro* and *in vivo* models of GBM. A large body of data now confirms the clinical safety of MRgFUS,[46,49,50] making this technology easier to translate to the patient. Our future work will examine the efficacy of FUS plus systemic administration of GNP-cisplatin conjugates for treatment of GBM, with the ultimate goal of assessing this treatment in clinical studies.

Acknowledgments

We would like to thank Stacey Krumholtz for the illustrations presented in this paper, and for the support of staff from the

Toronto Centre for Phenogenomics for the animal studies. We would also like to thank Brian Golbourn and Hidehiro Okura from the Rutka lab for their technical assistance.

Appendix A. Supplementary data

Supplementary data to this article can be found online at https://doi.org/10.1016/j.nano.2018.01.021.

References

1. Ostrom QT, Gittleman H, Liao P, Rouse C, Chen Y, Dowling J, et al. CBTRUS statistical report: primary brain and central nervous system tumors diagnosed in the United States in 2007-2011. *Neuro-Oncology* 2014;**16**(Suppl 4):iv1-63.
2. Stupp R, Mason WP, van den Bent MJ, Weller M, Fisher B, Taphoorn MJ, et al. Radiotherapy plus concomitant and adjuvant temozolomide for glioblastoma. *Med* 2005;**352**(10):987-96.
3. Deeken JF, Loscher W. The blood-brain barrier and cancer: transporters, treatment, and Trojan horses. *Clin Cancer Res* 2007;**13**(6):1663-74.
4. Daneman R. The blood-brain barrier in health and disease. *Ann Neurol* 2012;**72**(5):648-72.
5. Westphal M, Hilt DC, Bortey E, Delavault P, Olivares R, Warnke PC, et al. A phase 3 trial of local chemotherapy with biodegradable carmustine (BCNU) wafers (Gliadel wafers) in patients with primary malignant glioma. *J Neuro Oncol* 2003;**5**(2):79-88.
6. Mjos KD, Orvig C. Metallodrugs in medicinal inorganic chemistry. *Chem Rev* 2014;**114**(8):4540-63.
7. Boeckman HJ, Trego KS, Turchi JJ. Cisplatin sensitizes cancer cells to ionizing radiation via inhibition of nonhomologous end joining. *Mol Cancer Res* 2005;**3**(5):277-85.
8. Strumberg D, Brugge S, Korn MW, Koeppen S, Ranft J, Scheiber G, et al. Evaluation of long-term toxicity in patients after cisplatin-based chemotherapy for non-seminomatous testicular cancer. *Ann Oncol* 2002;**13**(2):229-36.
9. Ivanov AI, Christodoulou J, Parkinson JA, Barnham KJ, Tucker A, Woodrow J, et al. Cisplatin binding sites on human albumin. *J Biol Chem* 1998;**273**(24):14721-30.
10. Urien S, Lokiec F. Population pharmacokinetics of total and unbound plasma cisplatin in adult patients. *Clin Pharmacol* 2004;**57**(6):756-63.
11. Kim BY, Rutka JT, Chan WC. Nanomedicine. *Med* 2010;**363**(25):2434-43.
12. Butterworth KT, McMahon SJ, Currell FJ, Prise KM. Physical basis and biological mechanisms of gold nanoparticle radiosensitization. *Nanoscale* 2012;**4**(16):4830-8.
13. Davis ME, Zuckerman JE, Choi CH, Seligson D, Tolcher A, Alabi CA, et al. Evidence of RNAi in humans from systemically administered siRNA via targeted nanoparticles. *Nature* 2010;**464**(7291):1067-70.
14. Libutti SK, Paciotti GF, Byrnes AA, Alexander Jr HR, Gannon WE, Walker M, et al. Phase I and pharmacokinetic studies of CYT-6091, a novel PEGylated colloidal gold-rhTNF nanomedicine. *Clin Cancer Res* 2010;**16**(24):6139-49.
15. Arvizo RR, Saha S, Wang E, Robertson JD, Bhattacharya R, Mukherjee P. Inhibition of tumor growth and metastasis by a self-therapeutic nanoparticle. *S A* 2013;**110**(17):6700-5.
16. Kircher MF, de la Zerda A, Jokerst JV, Zavaleta CL, Kempen PJ, Mittra E, et al. A brain tumor molecular imaging strategy using a new triple-modality MRI-photoacoustic-Raman nanoparticle. *Nat Med* 2012;**18**(5):829-34.
17. Gaspar LE, Fisher BJ, Macdonald DR, LeBer DV, Halperin EC, Schold Jr SC, et al. Supratentorial malignant glioma: patterns of recurrence and implications for external beam local treatment. *Radiat Oncol Biol Phys* 1992;**24**(1):55-7.
18. Diaz RJ, McVeigh PZ, O'Reilly MA, Burrell K, Bebenek M, Smith C, et al. Focused ultrasound delivery of Raman nanoparticles across the blood-brain barrier: potential for targeting experimental brain tumors. *Nanomedicine* 2014;**10**(5):1075-87.
19. Etame AB, Diaz RJ, O'Reilly MA, Smith CA, Mainprize TG, Hynynen K, et al. Enhanced delivery of gold nanoparticles with therapeutic potential into the brain using MRI-guided focused ultrasound. *Nanomedicine* 2012;**8**(7):1133-42.
20. Burgess A, Nhan T, Moffatt C, Klibanov AL, Hynynen K. Analysis of focused ultrasound-induced blood-brain barrier permeability in a mouse model of Alzheimer's disease using two-photon microscopy. *J Control Release* 2014;**192**:243-8.
21. Xiong X, Arvizo RR, Saha S, Robertson DJ, McMeekin S, Bhattacharya R, et al. Sensitization of ovarian cancer cells to cisplatin by gold nanoparticles. *Oncotarget* 2014;**5**(15):6453-65.
22. Kalderon D, Roberts BL, Richardson WD, Smith AE. A short amino acid sequence able to specify nuclear location. *Cell* 1984;**39**(3 Pt 2):499-509.
23. Ragin AD, Morgan RA, Chmielewski J. Cellular import mediated by nuclear localization signal Peptide sequences. *Chem Biol* 2002;**9**(8):943-8.
24. Setua S, Ouberai M, Piccirillo SG, Watts C, Welland M. Cisplatin-tethered gold nanospheres for multimodal chemo-radiotherapy of glioblastoma. *Nanoscale* 2014;**6**(18):10865-73.
25. Siddik ZH. Cisplatin: mode of cytotoxic action and molecular basis of resistance. *Oncogene* 2003;**22**(47):7265-79.
26. Gately DP, Howell SB. Cellular accumulation of the anticancer agent cisplatin: a review. *Cancer* 1993;**67**(6):1171-6.
27. Chithrani BD, Ghazani AA, Chan WC. Determining the size and shape dependence of gold nanoparticle uptake into mammalian cells. *Nano Lett* 2006;**6**(4):662-8.
28. Albanese A, Tang PS, Chan WC. The effect of nanoparticle size, shape, and surface chemistry on biological systems. *Annu Rev Biomed Eng* 2012;**14**:1-16.
29. Alric C, Miladi I, Kryza D, Taleb J, Lux F, Bazzi R, et al. The biodistribution of gold nanoparticles designed for renal clearance. *Nanoscale* 2013;**5**(13):5930-9.
30. Ernsting MJ, Murakami M, Roy A, Li SD. Factors controlling the pharmacokinetics, biodistribution and intratumoral penetration of nanoparticles. *J Control Release* 2013;**172**(3):782-94.
31. Wang D, Lippard SJ. Cellular processing of platinum anticancer drugs. *Nat Rev Drug Discov* 2005;**4**(4):307-20.
32. Comenge J, Sotelo C, Romero F, Gallego O, Barnadas A, Parada TG, et al. Detoxifying antitumoral drugs via nanoconjugation: the case of gold nanoparticles and cisplatin. *PLoS One* 2012;**7**(10)e47562.
33. Mano M, Teodosio C, Paiva A, Simoes S, Pedroso de Lima MC. On the mechanisms of the internalization of S4(13)-PV cell-penetrating peptide. *Biochem J* 2005;**390**(Pt 2):603-12.
34. Sorkin A, Von Zastrow M. Signal transduction and endocytosis: close encounters of many kinds. *Nat Rev Mol Cell Biol* 2002;**3**(8):600-14.
35. Hynynen K, McDannold N, Vykhodtseva N, Jolesz FA. Noninvasive MR imaging-guided focal opening of the blood-brain barrier in rabbits. *Radiology* 2001;**220**(3):640-6.
36. Balasubramanian SK, Jittiwat J, Manikandan J, Ong CN, Yu LE, Ong WY. Biodistribution of gold nanoparticles and gene expression changes in the liver and spleen after intravenous administration in rats. *Biomaterials* 2010;**31**(8):2034-42.
37. Staedtke V, Bai RY, Laterra J. Investigational new drugs for brain cancer. *Expert Opin Investig Drugs* 2016;**25**(8):937-56.
38. Kumar A, Huo S, Zhang X, Liu J, Tan A, Li S, et al. Neuropilin-1-targeted gold nanoparticles enhance therapeutic efficacy of platinum(IV) drug for prostate cancer treatment. *ACS Nano* 2014;**8**(5):4205-20.
39. Yang C, Uertz J, Yohan D, Chithrani BD. Peptide modified gold nanoparticles for improved cellular uptake, nuclear transport, and intracellular retention. *Nanoscale* 2014;**6**(20):12026-33.
40. Dreaden EC, Austin LA, Mackey MA, El-Sayed MA. Size matters: gold nanoparticles in targeted cancer drug delivery. *Ther Deliv* 2012;**3**(4):457-78.

41. Kovacs Z, Werner B, Rassi A, Sass JO, Martin-Fiori E, Bernasconi M. Prolonged survival upon ultrasound-enhanced doxorubicin delivery in two syngenic glioblastoma mouse models. *J Control Release* 2014;**187**:74-82.
42. Treat LH, McDannold N, Zhang Y, Vykhodtseva N, Hynynen K. Improved anti-tumor effect of liposomal doxorubicin after targeted blood-brain barrier disruption by MRI-guided focused ultrasound in rat glioma. *Ultrasound Med Biol* 2012;**38**(10):1716-25.
43. Wei KC, Chu PC, Wang HY, Huang CY, Chen PY, Tsai HC, et al. Focused ultrasound-induced blood-brain barrier opening to enhance temozolomide delivery for glioblastoma treatment: a preclinical study. *PLoS One* 2013;**8**(3)e58995.
44. Elias WJ, Huss D, Voss T, Loomba J, Khaled M, Zadicario E, et al. A pilot study of focused ultrasound thalamotomy for essential tremor. *Med* 2013;**369**(7):640-8.
45. Marquet F, Tung YS, Teichert T, Ferrera VP, Konofagou EE. Noninvasive, transient and selective blood-brain barrier opening in non-human primates in vivo. *PLoS One* 2011;**6**(7)e22598.
46. Carpentier A, Canney M, Vignot A, Reina V, Beccaria K, Horodyckid C, et al. Clinical trial of blood-brain barrier disruption by pulsed ultrasound. *Sci Transl Med* 2016;**8**(343):343re2, https://doi.org/10.1126/scitranslmed.aaf6086.
47. Jacobs S, McCully CL, Murphy RF, Bacher J, Balis FM, Fox E. Extracellular fluid concentrations of cisplatin, carboplatin, and oxaliplatin in brain, muscle, and blood measured using microdialysis in nonhuman primates. *Cancer Chemother Pharmacol* 2010;**65**(5):817-24.
48. Chithrani DB, Jelveh S, Jalali F, van Prooijen M, Allen C, Bristow RG, et al. Gold nanoparticles as radiation sensitizers in cancer therapy. *Radiat Res* 2010;**173**(6):719-28.
49. Coluccia D, Fandino J, Schwyzer L, O'Gorman R, Remonda L, Anon J, et al. First noninvasive thermal ablation of a brain tumor with MR-guided focused ultrasound. *J Ther Ultrasound* 2014;**2**:17.
50. Monteith S, Sheehan J, Medel R, Wintermark M, Eames M, Snell J, et al. Potential intracranial applications of magnetic resonance-guided focused ultrasound surgery. *J Neurosurg* 2013;**118**(2):215-21.
51. Timbie KF, Afzal U, Date A, Zhang C, Song J, Wilson Miller G, et al. MR image-guided delivery of cisplatin-loaded brain-penetrating nanoparticles to invasive glioma with focused ultrasound. *J Control Release* 2017;**263**:120-31.